Variation of Transition-State Structure as a Function of the Nucleotide in Reactions Catalyzed by Dehydrogenases. 2. Formate Dehydrogenase†

Jeffrey D. Hermes, Scott W. Morrical, Marion H. O'Leary, and W. W. Cleland*

ABSTRACT: Since hydride transfer is completely rate limiting for yeast formate dehydrogenase [Blanchard, J. S., & Cleland, W. W. (1980) *Biochemistry 19*, 3543], the intrinsic isotope effects on this reaction are fully expressed. Primary deuterium, ^{13}C, and ^{18}O isotope effects in formate and the α-secondary deuterium isotope effect at C-4 of the nucleotide have been measured for nucleotide substrates with redox potentials varying from −0.320 (NAD) to −0.258 V (acetylpyridine–NAD). As the redox potential gets more positive, the primary deuterium isotope effect increases from 2.2 to 3.1, the primary ^{13}C isotope effect decreases from 1.042 to 1.036, the α-secondary deuterium isotope effect drops from 1.23 to 1.06, and V_{max} decreases. The ^{18}O isotope effects increase from 1.005 to 1.008 per single ^{18}O substitution in formate (these values are dominated by the normal isotope effect on the dehydration of formate during binding; pyridinealdehyde–NAD gives an inverse value, possibly because it is not fully dehydrated during binding). These isotope effects suggest a progression toward earlier transition states as the redox potential of the nucleotide becomes more positive, with NAD having a late and acetylpyridine–NAD a nearly symmetrical transition state. By contrast, the I_2 oxidation of formate in dimethyl sulfoxide has a very early transition state (^{13}k = 1.0154; ^{D}k = 2.2; ^{18}k = 0.9938), which becomes later as the proportion of water in the solvent increases (^{13}k = 1.0265 in 40% dimethyl sulfoxide and 1.0362 in water). α-secondary deuterium isotope effects with formate dehydrogenase are decreased halfway to the equilibrium isotope effect when deuterated formate is the substrate, showing that the bending motion of the secondary hydrogen is coupled to hydride transfer in the transition state and that tunneling of the two hydrogens is involved. The ^{15}N isotope effect of 1.07 for NAD labeled at N-1 of the nicotinamide ring suggests that N-1 becomes pyramidal during the reaction. ^{18}O fractionation factors for formate ion relative to aqueous solution are 1.0016 in sodium formate crystal, 1.0042 bound to Dowex-1, and 1.0040 as an ion pair (probably hydrated) in $CHCl_3$. The CO_2 analogue azide binds about 10^4 times better than the formate analogue nitrate to enzyme–nucleotide complexes (even though the K_i values for both and the affinity for formate vary by 2 orders of magnitude among the various nucleotides), but the ratio is not sensitive to the redox potential of the nucleotide. Thus, not the nature of the transition state but rather the shape of the initial binding pocket for formate is determining the relative affinity. The change in transition-state structure as the nucleotide is altered must therefore be the result of the redox difference, rather than any differences in binding of reactants.

Yeast formate dehydrogenase (formate:NAD^+ oxidoreductase, EC 1.2.1.2) catalyzes the oxidation of formate to CO_2 with concomitant reduction of NAD to NADH:

$$NAD^+ + HCO_2^- \rightarrow CO_2 + NADH \quad (1)$$

The enzyme exists as a dimer of 42 000-dalton subunits and has no apparent metal ion requirement. By use of initial velocity studies, Blanchard & Cleland (1980) established the kinetic mechanism as ordered, with NAD adding before formate. Primary deuterium and ^{13}C isotope effects in formate were determined with both NAD and acetylpyridine–NAD. The ^{13}C isotope effect was identical with unlabeled and deuterated formate [although $^{D}(V/K)$ was 2.8], showing that all isotope effects measured were intrinsic ones on the chemical step of hydride transfer. Formate dehydrogenase is therefore ideally suited for study of transition-state properties. In the present paper we report the primary and α-secondary deuterium, primary ^{13}C (in formate), and ^{18}O isotope effects determined with NAD and its thio, acetylpyridine, and pyridinealdehyde analogues and attempt to deduce the variation in transition-state structure as a function of the redox potential of the nucleotide (see Figure 1). We also compare the primary deuterium, ^{13}C, and ^{18}O isotope effects with those for the chemical oxidation of formate by I_2 in dimethyl sulfoxide, water, or mixtures of the two. On the basis of the effect of primary deuterium substitution on the α-secondary deuterium isotope effect, we speculate regarding the shape of the potential barrier and the involvement of quantum mechanical tunneling in the reaction.

Materials and Methods

Chemicals. Yeast formate dehydrogenase and NAD (Li salt, formate free) were from Boehringer-Mannheim. Yeast and horse liver alcohol dehydrogenases, yeast aldehyde dehydrogenase, rabbit muscle lactate dehydrogenase, beef glutamate dehydrogenase, and carbonic anhydrase were from Sigma. Acetylpyridine–NAD and deamino-NAD were from P-L Biochemicals, while thio-NAD, pyridinealdehyde–NAD, nicotinic acid dinucleotide, and 3-amino-NAD were from Sigma. Sodium formate-*d* (99 atom % D), ethanol-d_6 (99 atom % D), [^{13}C]formic acid (90 atom % ^{13}C), [^{12}C]formic acid (99.9 atom % ^{12}C), and $H_2{}^{18}O$ (98 atom % ^{18}O) were from Merck. 3-Cyano-NAD was prepared from thio-NAD by treatment with methanolic silver nitrate according to the procedure of Biellmann & Jung (1970). Successful synthesis was confirmed by reaction with yeast alcohol dehydrogenase and ethanol to produce an appropriate λ_{max} (324 nm) for the reduced analogue. NAD containing ^{15}N at N-1 of the nicotinamide ring was a gift from Dr. Norman Oppenheimer.

Nomenclature. The nomenclature used is that of Northrop (1977), in which isotope effects on kinetic or thermodynamic parameters are indicated by leading superscripts. Thus, 13, 15, 18, T, D, or α-D refer to ^{13}C, ^{15}N, ^{18}O, tritium, primary deuterium, or α-secondary deuterium isotope effects. Where necessary, following subscripts are used. For example,

† From the Departments of Biochemistry and Chemistry, University of Wisconsin, Madison, Wisconsin 53706. *Received February 13, 1984.* Supported by a grant from the National Institutes of Health (GM 18938).

0006-2960/84/0423-5479$01.50/0

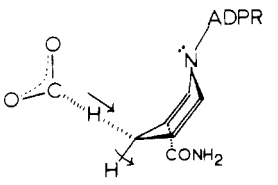

FIGURE 1: Transition state for the formate dehydrogenase reaction. Isotope effects have been measured for the atoms shown as letters (except for $CONH_2$ and ADPR). The geometry of the nicotinamide ring is hypothetical but is consistent with the observed ^{15}N isotope effect and with hydride transfer to the axial position at C-4.

$^{13}(V/K)_{formate\text{-}d}$ is the ^{13}C isotope effect of V/K with deuterated formate as substrate. For a further discussion of nomenclature, see Cook & Cleland (1981).

[$^{13}C^{18}O_2$]Formate. Conditions required for the oxygen exchange of formic acid were established with ^{13}C NMR (Risley & van Etten, 1980). Complete exchange of 20 μL of formic acid in 1.5 mL of 30 atom % $H_2{}^{18}O$ occurred within 4 days at room temperature; 20 μL of [^{13}C]formic acid was then added to 1.0 mL of $H_2{}^{18}O$ (98 atom % ^{18}O) in a 5-mm NMR tube equipped with a flea magnetic stir bar. The solution was tightly stoppered and mixed for 9 days at room temperature. After end-point assay for formic acid with formate dehydrogenase, 1.1 equiv of tripotassium phosphate was added, and the solvent was removed by a slow stream of N_2 to a trap cooled by liquid nitrogen. A total of 1.0 mL of D_2O was added for field lock, the stir bar was removed, and a limited acquisition ^{13}C NMR spectrum revealed one peak at a chemical shift of 166.0 ppm with a shoulder downfield by 0.023 ppm. The ratio of $^{18}O_2/^{18}O^{16}O/^{16}O_2$ was 95/5/ undetected. The formate concentration of this solution was determined by end-point assay, and it was mixed with [^{12}C]formic acid (99.9 atom % ^{12}C) in 100 mM K-Hepes, pH 8.0, to yield 500 mL of a solution 20 mM in formate with a natural abundance $^{13}C/^{12}C$ ratio (approximately 1.1%).

NAD-4-d. A combination of published techniques was used to synthesize NAD-*4-d* (Viola et al., 1979; Cook et al., 1980). In a 50-mL beaker equipped with a flea stir bar was placed 196 mg (0.28 mmol) of NAD (Li salt) in 15.0 mL of 6 mM Taps,[1] pH 9.0. To this was added 18 μL of ethanol-d_6 (0.35 mmol). KOH (0.1 N) was added along with 11.1 mg (100 units) of yeast aldehyde dehydrogenase and 56 mg (100 units) of horse liver alcohol dehydrogenase to maintain pH, which was kept at 9.0 during the reaction. After 1 h, at which time the A_{340} was constant and appropriate for 100% conversion to A-side NADD, 250 mg of $(NH_4)_2SO_4$ was added while the pH was maintained above 8.0. A total of 2000 units of glutamate dehydrogenase was then added, followed by 400 mg of α-ketoglutaric acid in 10-mg portions with pH adjustment after each addition. After 1 h (or until no further decrease in A_{340} was seen), the solution was centrifuged to remove any precipitated protein, and the supernatant was filtered through an Amicon PM-30 membrane at 40 psi of N_2 and 4 °C. The volume was reduced to 5 mL with a rotary evaporator, and the solution was applied to a 190 × 2 cm column of Sephadex G-10 equilibrated with 20 mM KCl and eluted with the same solution at 4 °C. The fractions absorbing at 260 nm were pooled, concentrated, and used for determinations of α-secondary isotope effects. The UV spectrum showed no detectable absorbance above 290 nm. Enzymatic end-point assays indicated a 70% recovered yield of NAD-*4-d* from NAD.

The 4-deuterated analogues of NAD were synthesized enzymatically in similar fashion with the following modifications: (1) twice the enzyme concentrations were used, (2) the appropriate wavelength for each reduced nucleotide was monitored (acetylpyridine–NADH, 363 nm; thio-NADH, 395 nm; pyridinealdehyde–NADH, 358 nm), and (3) HPLC purification for the thio and pyridinealdehyde analogues was employed by using a Waters reverse-phase (C-18) semiprep column (7.9 mm × 30 cm) with 30 mM phosphate, pH 6.0, as eluant at a flow rate of 3.0 mL/min.

Initial Velocity Studies. Initial velocities were measured by monitoring the appearance of NADH at 340 nm in either a Cary 118 or Beckman DU plus Gilford OD converter. Yeast formate dehydrogenase is inhibited by NADH (K_i = 6 μM). In order to ensure that initial velocities could be obtained from chart traces, a full scale of 0.02 *A* was used in all studies with NAD or NAD-*4-d*. All additions of less than 50 μL were made by using micropipets (Dade Diagnostics), and 3.0-mL cuvettes were used. Reactions were initiated by addition of a small volume of cold enzyme with an adder mixer. Reactions where NAD levels were varied at low formate concentrations were carried out in 5- or 10-cm cuvettes.

For determinations of α-secondary deuterium isotope effects, commercial formate dehydrogenase was purified from any contaminating nucleotide or formate by application of 180 units to a 190 × 2 cm column of Sephadex G-10 and elution with 10 mM Hepes, pH 7.8. All substrate and enzyme solutions were Millipore filtered to remove dust particles before use in these experiments.

Temperature was maintained to ±0.1 °C between 9 and 35 °C for the determination of activation energies for V and V/K. The enzyme activity was stable over the measurement period at all temperatures.

Determination of Substrate Concentrations. All substrate concentrations were determined enzymatically. Nucleotide concentrations were determined by using 10 units of horse liver alcohol dehydrogenase and 50 mM cyclohexanol in 100 mM Ches buffer, pH 9.5. Standard deviations in end-point assays for nucleotides were less than 0.5%. Formate solutions were calibrated to within 2% agreement with formate dehydrogenase and excess NAD in 100 mM Hepes, pH 7.8, with 35% dimethyl sulfoxide, which reduces product inhibition by NADH, thus giving a convenient, time-saving end-point analysis for formate. Since V/K isotope effects determined by direct comparison of the initial velocities with labeled and unlabeled substrates are only as precise as the substrate concentration calibrations, this point is critical. Blanchard & Cleland (1980) reported $^{D}(V/K_{formate})$ values that differ from those in the present work, presumably because of incorrectly calibrated formate solutions.

Determination of Formate Dehydrogenase ^{13}C Isotope Effects. The technique employed for determination of ^{13}C isotope effects is that described in detail by O'Leary (1980) in which the natural abundance of ^{13}C in formate is used as a trace label to minimize errors caused by contamination with atmospheric CO_2. Reaction mixtures for low conversion contained 20 mM formate, 0.5 mM NAD or analogue, and 22 mM pyruvate (used with lactate dehydrogenase to reoxidize the NADH produced from the formate dehydrogenase reaction) in a total volume of 20 mL. Complete conversion solutions (15 mL) contained 6.7 mM formate, 7.33 mM pyruvate, and 0.5 mM NAD. Complete conversion samples were always analyzed on the same day as low conversion reactions, and NAD was always used as the oxidant. The solutions were

[1] Abbreviations: Hepes, *N*-(2-hydroxyethyl)piperazine-*N*'-2-ethanesulfonate; Taps, 3-[[tris(hydroxymethyl)methyl]amino]propanesulfonate; Ches, 2-(*N*-cyclohexylamino)ethanesulfonate; HPLC, high-pressure liquid chromatography.

initially degassed with CO_2-free N_2 for 4 h at pH 5. After adjustment of the pH to 7.8 with saturated KOH, the buffer containing formate, pyruvate, and NAD was degassed for an additional 8 h. After temperature equilibration to 25 °C, 7 mg (0.3 unit/mg lyophilysate) of formate dehydrogenase and 1 mg (700 units/mg) of lactate dehydrogenase were introduced into the reaction vessel in 0.1 mL of CO_2-free buffer with a syringe. Low conversion reactions were quenched at time periods of from 30 min (NAD) to 20 h (pyridinealdehyde–NAD) by using 0.4 mL of concentrated H_2SO_4. In the reactions with pyridinealdehyde–NAD the formate concentration was increased to 300 mM and the nucleotide concentration to 1 mM (at least 20 μmol of CO_2 is needed for determination of $^{13}C/^{12}C$ ratios on the RMS 6-60 isotope ratio mass spectrometer). The 100% conversions were allowed to react for 24 h.

To isolate the CO_2, a series of freeze, distillation, and thaw procedures were utilized. First, N_2 was removed from the system by freezing the reaction vessels in liquid N_2 (CO_2 condenses) and venting on a vacuum line. This process was repeated 4 times with complete thaws in between. Second, the CO_2 contained in the reaction vessel was distilled from a dry ice–2-propanol bath to a liquid nitrogen cooled collection tube. Five such distillations, with complete thawing in between, were sufficient to remove all CO_2 from the reaction solution. Since this CO_2 can be somewhat wet, four additional bulb-to-bulb distillations from dry ice–2-propanol baths were used to dry the CO_2 suitably for mass spectrometry. To determine the extent of reaction, the CO_2 was measured manometrically.

The isotopic composition of the CO_2 was determined on an isotope ratio mass spectrometer (either a Nuclide Associates RMS 6-60 with a manual leak control rate or a Varian MAT 250). Measurements were carried out within 24 h of isolation of CO_2 samples to minimize atmospheric leaks into the sample storage tubes.

Determination of ^{18}O Kinetic Isotope Effects. ^{18}O isotope effects were determined by the remote label method of O'Leary & Marlier (1979) in which the apparent ^{13}C isotope effect was measured for a 90:1 mixture of $H^{12}C^{16}O_2^-$ and $H^{13}C^{18}O_2^-$. This apparent isotope effect is the product of the ^{13}C isotope effect and the square of the ^{18}O isotope effect and in conjunction with the measured ^{13}C isotope effect can be used to calculate the actual ^{18}O isotope effect as described under Data Analysis. The enzyme incubations and procedures were identical with those described for determination of the ^{13}C isotope effects except that 20 mM [$^{13}C^{18}O_2$,$^{12}C^{16}O_2$]formate was used, the degassing at pH 5 was replaced by degassing at pH 7.8 to avoid washout of ^{18}O, and carbonic anhydrase was included in both the low conversion and complete conversion samples to ensure that CO_2 equilibration with the solvent was complete prior to isotopic analysis.[2] To confirm that equilibration of the product $C^{18}O_2$ with solvent ^{16}O had occurred in the initial ^{18}O isotope effect determinations with NAD as the nucleotide, the CO_2 isolated was analyzed by mass spectrometry, put back over H_2O and shaken for 24 h, and then reanalyzed. This procedure gave no change in the $^{13}C/^{12}C$ ratio.

Determination of $^{18}K_{eq}$ for Formic Acid Equilibration with H_2O. Formic acid (104 μL) was equilibrated for 2 weeks with 5 mL of H_2O adjusted to pH 1.5 with 12 N HCl. Neutralization with KOH, lyophilization, and oxidation by I_2 in dimethyl sulfoxide (see below) yielded CO_2 with the same ^{18}O composition as that of the equilibrated formic acid. To determine the ^{18}O content of the water, a sample of the original formic acid (thus keeping the same ^{13}C content) was converted to CO_2 in this water by formate dehydrogenase. Acidification before isolation established the CO_2–H_2O equilibrium.

Iodine Oxidation of Formate in Dimethyl Sulfoxide. The quantitative oxidation of formate to CO_2 by iodine occurs at room temperature in either water or dimethyl sulfoxide, but reaction in the latter is $\sim 10^7$ times faster than in water (Hiller & Krueger, 1967) and allows isolation of CO_2 without exchange of oxygen with a solvent. Typically, a 10-fold excess of I_2 (freshly sublimed) was used with 1 equiv of anhydrous sodium acetate to neutralize the HI generated during the reaction. A reaction vessel with side bulb for I_2 was utilized for degassing the dimethyl sulfoxide–formate solution. I_2 was mixed with the dimethyl sulfoxide–formate solution after complete degassing (3-h sparge with CO_2-free N_2). A small stir bar was used for mixing, and all reactions were allowed to proceed overnight. By manometric measurement, the yields of CO_2 were quantitative. The freeze–thaw procedure outlined for isolated of CO_2 from aqueous solution is convenient for the isolation from dimethyl sulfoxide, also. Dimethyl sulfoxide used for the experiments was distilled from KOH at 10 mmHg (80 °C) and kept dry by storage over 4-Å molecular sieves.

Determination of ^{13}C Isotope Effects for the Iodine Oxidation of Formate. The ^{13}C isotope effects for this chemical reaction were determined in the usual fashion (O'Leary, 1980) in which CO_2 produced from 10% and 100% reactions is analyzed for $^{13}C/^{12}C$ ratio with a slight modification. Since the bimolecular rate constant is large enough (Hiller & Krueger, 1967) to preclude possible quenching after low percent reaction, an alternate procedure for stopping the reaction at fractional consumption of formate was required. The technique used was to limit the level of iodide so that exhaustion of oxidizing equivalents stopped the reaction. In the complete conversion reactions a 3-fold excess of iodine was used, and dimethyl sulfoxide was always used as the solvent to ensure 100% conversion to CO_2.

After the solution was vigorously stirred for 1 h, 230 mg of potassium formate completely dissolved in 100 mL of dry dimethyl sulfoxide. Aliquots (20 mL for the low conversion and 5 mL for the 100% conversion) were degassed with CO_2-free N_2 for 1 h. To the side bulbs of the reaction vessels were added 15 mg (low conversion) or 250 mg of iodine (100% reaction). After an additional 10 min of degassing, the iodine was mixed with the solution and allowed to react for 5.5 h.

For determinations in aqueous solutions or 40% mole fraction of dimethyl sulfoxide, the above procedure was followed except that 100 mM phosphate, pH 7.35, was used and 50 mg of KI was added to the I_2 in the side bulb.

Isolation of CO_2 was accomplished in the usual fashion with a series of liquid nitrogen freeze–thaws followed by 2-propanol/dry ice freeze–thaws and bulb to bulb distillations.

Data Analysis. Reciprocal initial velocities were plotted vs. the reciprocals of substrate concentrations, and the data were fitted to the appropriate rate equations by the least-squares method, assuming equal variances for either v or log v, using a digital computer and the Fortran programs of Cleland (1979). Individual saturation curves were fitted to eq 2, where

$$v = VA/(K + A) \quad (2)$$

v is the maximum velocity, A is the substrate concentration, and K is the Michaelis constant. Competitive inhibition data were fitted to eq 3 where K_i is the slope inhibition constant

[2] Only the m/e 45/44 ($^{13}C^{16}O_2/^{12}C^{16}O_2$) isotope ratio was used to determine the ^{18}O isotope effects. Therefore, any ^{18}O-labeled $^{13}CO_2$ resulting from the enzymatic reaction must be thoroughly equilibrated with $H_2{}^{16}O$.

$$v = VA/[K(1 + I/K_i) + A] \quad (3)$$

and I the inhibitor concentration. For analysis of primary deuterium isotope effects determined by varying the concentration of protioformate or deuterated formate at saturating levels of NAD, initial velocities were fitted to eq 4 or 5, which

$$v = VA/[K(1 + F_iE_{V/K}) + A(1 + F_iE_V)] \quad (4)$$

$$v = VA/[(K + A)(1 + F_iE_{V/K})] \quad (5)$$

assumes independent or equal isotope effects on V and V/K. In eq 4 and 5 F_i is the fraction of deuterium label in the substrate, while $E_{V/K}$ and E_V are the isotope effect minus one on the subscripted parameter. The best fit of the experimental data was taken as that with the lowest value of σ (sum of squares of the residuals divided by the degrees of freedom).

Secondary deuterium isotope effects were obtained by fitting the initial velocities to either eq 4 or eq 5 when the formate concentration was varied at saturating nucleotide or deuterated nucleotide levels or to eq 5 when nucleotide or deuterated nucleotide concentrations were varied at a formate level one-tenth of $K_{formate}$. Since formate dehydrogenase has an ordered kinetic mechanism with NAD adding first, the initial velocity experiment performed in this manner yields the α-secondary isotope effect on V/K from both the slope and intercept ratios of the reciprocal plots.

The $^{13}(V/K)$ and $^{13,18,18}(V/K)$ isotope effects were computed from eq 6:

$$^{13}(V/K) \text{ or } ^{13,18,18}(V/K) = \frac{\log (1 - f)}{\log (1 - fR/R_0)} \quad (6)$$

where R_0 and R are the $^{13}C/^{12}C$ isotope ratios in the initial substrate (measured in product at $f = 1.0$) and product at fractional conversion f. The $^{18}(V/K)$ isotope effect for a single ^{18}O is then

$$^{18}(V/K) = \sqrt{^{13,18,18}(V/K)/^{13}(V/K)} \quad (7)$$

if double labeling is complete (that is, only two species of formate exist: $H^{13}C^{18}O_2^-$ and $H^{12}C^{16}O_2^-$).

However, the formate used to determine the ^{18}O isotope effects had the following composition: $^{13}C^{18}O_2$, 1.187%; $^{13}C^{18}O^{16}O$, 0.063%; $^{12}C^{18}O_2$, 0.119%; $^{12}C^{16}O_2$, 98.631%. Because this problem will arise in all work with the remote label method, we develop the exact equations needed for this situation. The double-labeled formate actually contains three species that are significant: $H^{13}C^{18}O_2^-$, $H^{13}C^{18}O^{16}O^-$, and $H^{12}C^{18}O_2^-$ (the level of $H^{12}C^{18}O^{16}O^-$ or of any $^{16}O_2$ species is negligible). If x is the fraction of ^{13}C, y is the fraction of $^{18}O_2$ in the mixture ($1 - y$ is the fraction of $^{18}O^{16}O$ labeling), and b is the fraction of this mixture in the final formate (bx should approximate the natural abundance of the remote label, which is ^{13}C in this case, in order to minimize errors from contamination), the proportions of these species in the final formate mixture used for the experiments are given by

$$H^{13}C^{18}O_2^- = bxy$$

$$H^{13}C^{18}O^{16}O^- = bx(1 - y)$$

$$H^{12}C^{18}O_2^- = b(1 - x)y$$

The [^{12}C]formate contains two significant species ($H^{13}C^{18}O^{16}O^-$ or species containing $^{18}O_2$ are insignificant), while $H^{12}C^{18}O^{16}O^-$, while present at about 0.2% because of the natural abundance of ^{18}O, has a negligible effect on observed isotope effects and will not be further considered. If z is the ^{13}C abundance in the [^{12}C]formate, we have

$$H^{12}C^{16}O_2^- = (1 - b)(1 - z)$$

$$H^{13}C^{16}O_2^- = (1 - b)z$$

Although the $H^{12}C^{18}O_2^-$ is 10% of the double-labeled formate and about 0.1% of the total final formate, its effect on the isotope effect is negligible, and it can be ignored. The $^{13}C/^{12}C$ ratio in the formate used for the experiments is thus

$$\frac{bxy + bx(1 - y) + (1 - b)z}{(1 - b)(1 - z)} \quad (8)$$

The corresponding ratio in the first product produced is given by

$$[bxy/[^{13}k(^{18}k)^2] + bx(1 - y)/(^{13}k^{18}k) + (1 - b)z/^{13}k]/[(1 - b)(1 - z)] \quad (9)$$

where ^{13}k and ^{18}k are isotope effects caused by ^{13}C and single ^{18}O substitution. The observed value of the isotope effect, which is based solely on the $^{13}C/^{12}C$ ratio in the product CO_2, since the ^{18}O in the product is restored to natural abundance by equilibration with water, is then given by

$$^{13,18,18}(V/K) = \frac{bxy + bx(1 - y) + (1 - b)z}{bxy/[^{13}k(^{18}k)^2] + bx(1 - y)/(^{13}k^{18}k) + (1 - b)z/^{13}k} = \frac{^{13}k(^{18}k)^2[1 + (1 - b)z/(bx)]}{1 + (^{18}k - 1)(1 - y) + (1 - b)z(^{18}k)^2/(bx)} \quad (10)$$

from which

$$^{18}k = \sqrt{\frac{^{13,18,18}(V/K)[1 + (^{18}k - 1)(1 - y)]}{^{13}k - [(1 - b)z/(bx)][^{13,18,18}(V/K) - ^{13}k]}} \quad (11)$$

This equation contains ^{18}k on the right side, but because of the near identity

$$\sqrt{1 + (^{18}k - 1)(1 - y)} \simeq 1 + (^{18}k - 1)(1 - y)/2 \quad (12)$$

it is possible to rearrange eq 11 to[3]

$$^{18}k = 1 + \left[\sqrt{\frac{^{13,18,18}(V/K)}{^{13}k - [(1 - b)z/(bx)](^{13,18,18}(V/K) - ^{13}k)}} - 1\right] \times [1 + (1 - y)/2] \quad (13)$$

It is clear from the form of eq 13 that it reduces to eq 7 if $y = 1$ and $z = 0$. The value of x is not critical and, in fact, will not matter at all if $z = 0$. While y has an effect, the percent error in $^{18}k - 1$ is only $50(1 - y)$, or 2.5% in the present case, if the last term in eq 13 is dropped. What is critical, however, is the value of z. If the [^{12}C]formate contains an appreciable level of ^{13}C, the denominator under the square root sign is significantly affected, especially if x is not close to unity. It is thus important to have as pure a ^{12}C sample as possible to use for mixing with the $^{13}C^{18}O_2$-labeled formate. Equation 13 thus makes clear the principles involved in the remote label method (O'Leary & Marlier, 1979), namely, the following: (1) The remote label which is used to follow isotope discrimination is reconstituted from the light isotope with as low as possible a content (but measured!) of the heavy one and a

[3] An exact rearrangement of eq 11 when eq 12 is substituted in it gives the reciprocal of $[1 - (1 - y)\sqrt{}/2]$ as the last term in eq 13, where $\sqrt{}$ is the square root term in eq 13, but the form shown gives $^{18}k - 1$ values accurate to within 1% and is simpler to use.

Table I: Kinetic Parameters for Nucleotide Substrates of Formate Dehydrogenase at pH 7.8, 25 °C

nucleotide	$E^{\circ\prime}$ (V), pH 7	K_m (μM)	$K_{formate}$ (mM)	relative		activation energy (kcal/mol)	
				V_{max}	$V/K_{formate}$	V_{max}	$V/K_{formate}$
NAD	−0.320	32	2.7	(100)	(100)	16.2 ± 0.2	7.6 ± 0.3
deamino-NAD[a]	−0.320	540	4.9	100	35	ND[c]	ND
thio-NAD	−0.285	170	38	89	20	16.8 ± 0.6	12.9 ± 0.5
pyridinealdehyde–NAD	−0.262	190	84	0.05	0.003	23.5 ± 1.5	16.9 ± 0.8
acetylpyridine–NAD	−0.258	1160	294	4	0.02	ND	10.9 ± 0.3[b]

[a] Adenine replaced by hypoxanthine. [b] Determined by Blanchard & Cleland (1980). [c] ND, not determined.

Table II: Inhibition Constants for Nitrate and Azide as Competitive Inhibitors of Formate Dehydrogenase[a]

nucleotide	$K_{i\,nitrate}$ (mM)	$K_{i\,azide}$ (μM)	($K_{i\,azide}/K_{i\,nitrate}$) × 10^4	$K_{formate}/K_{i\,nitrate}$
NAD	0.35 ± 0.02	0.075 ± 0.019	2.1	7.7
thio-NAD	13 ± 2	1.6 ± 0.1	1.2	2.9
acetylpyridine–NAD	34 ± 5	2.7 ± 0.3	0.8	8.6
pyridinealdehyde–NAD	5.2 ± 0.4	9.6 ± 0.6	18	16

[a] pH 7.8, 100 mM Hepes. Formate concentrations were varied at fixed levels of nucleotide (>5K_m, except 2.5K_m for acetylpyridine–NAD).

Table III: Primary Deuterium Isotope Effects with Formate Dehydrogenase[a]

nucleotide	fit to eq 4		fit to eq 5
	^{D}V	$^{D}(V/K_{formate})$	$^{D}(V/K) = {}^{D}V$
NAD	2.13 ± 0.09	2.27 ± 0.21	2.17 ± 0.04
deamino-NAD	1.5 ± 0.4	2.40 ± 0.22	2.14 ± 0.08
thio-NAD	2.95 ± 0.03	2.36 ± 0.21	2.60 ± 0.07
pyridinealdehyde–NAD	2.83 ± 0.38	2.86 ± 0.14	2.85 ± 0.04
acetylpyridine–NAD	−5.9 ± 6.8	3.12 ± 0.14	3.32 ± 0.05

[a] pH 7.8, 25 °C. Nucleotide concentrations were constant at >10K_m (except for 2K_m for acetylpyridine–NAD). The concentrations of formate or deuterated formate were varied and the initial velocities fitted to eq 4 or 5.

Table IV: α-Secondary Deuterium Isotope Effects with Formate Dehydrogenase[a]

nucleotide	procedure[b]	$^{\alpha\text{-}D}(V/K_{formate})$[c]	
		formate	formate-*d*
NAD	I	1.23 ± 0.03	1.07 ± 0.02
	I	1.23 ± 0.02	1.06 ± 0.01
	II	1.21 ± 0.01	1.07 ± 0.01
NAD at 6.5 °C	I	1.22 ± 0.01	1.08 ± 0.01
thio-NAD	II	1.18 ± 0.02	1.03 ± 0.01
acetylpyridine–NAD	II	1.06 ± 0.03	0.95 ± 0.02
pyridinealdehyde–NAD	II	0.99 ± 0.01	0.94 ± 0.02

[a] pH 7.8, 25 °C (except where noted). [b] (I) Formate concentrations were varied at fixed (20 K_m) levels of NAD or NAD-*4-d*. (II) The level of NAD or NAD-*4-d* was varied at one-tenth the K_m level of formate. [c] Data fitted to eq 5, which assumes equal isotope effects on slopes and intercepts.

double-labeled sample of heavy isotope, with the two mixed in such a ratio that the final mass ratio is as close as possible to the natural abundance level. (2) The natural abundance of the heavy isotope causing the desired discrimination causes no problems (for D, ^{13}C, ^{15}N, or ^{18}O), and the degree of labeling in the double-labeled species is not critical but should be as high as possible and accurately measured. (3) The isotope effect caused by the remote label itself must be separately determined with the natural abundance label and corrected for by eq 13 or where discrimination is by a single, rather than by a double, label, by eq 14 (where y is now the fraction of label in the single position causing discrimination):[4]

$$^{18}k = \frac{^{13,18}(V/K)y}{^{13}k - [^{13,18}(V/K) - {}^{13}k][(1-b)z/(bx)] - {}^{13,18}(V/K)(1-y)} \quad (14)$$

Most cases, in fact, will involve use of eq 14 rather than eq 13.

For the present work, the values for ^{13}k were from Table V. The values for b, x, y, and z were 0.01369, 0.90, 0.95, and 0.0032.

Results

Nucleotide Specificity of Formate Dehydrogenase. The kinetic parameters for NAD analogues that are substrates are listed in Table I. Nicotinic acid dinucleotide, 3-amino-NAD, and 3-cyano-NAD showed no activity (<0.004% that of NAD) at concentrations of 5 mM nucleotide and 20 mM formate. A mixture of nicotinamide mononucleotide (5 mM) and AMP (0.5 mM) did not replace NAD.

Temperature Dependence of V and $V/K_{formate}$. These parameters were determined at 9, 18, 26, and 35 °C by varying formate at saturating levels of NAD, thio-NAD, or pyridinealdehyde–NAD. The K_m for acetylpyridine–NAD is too high to allow precise determinations of V. The activation energies in Table I were calculated from Arrhenius plots.

Inhibition by Nitrate and Azide. Competitive inhibition constants for nitrate and azide were determined with NAD, thio-NAD, acetylpyridine–NAD, and pyridinealdehyde–NAD as the nucleotide substrates and formate as the variable substrate. These values are in Table II.

Primary Deuterium Isotope Effects. When the concentration of formate-(H,*d*) was varied at high fixed levels of NAD, thio-NAD, or pyridinealdehyde–NAD, the primary deuterium isotope effects of V/K and V in Table III were obtained. With acetylpyridine–NAD only twice K_m levels could be used because of the high K_m (1.16 mM). This could cause the apparent ^{D}V to be in error, but the value of $^{D}(V/K_{formate})$ will be correct. It appears that equal isotope effects are seen on V/K and V when those on the latter can be determined with any precision.

α-Secondary Deuterium Isotope Effects. When the level of formate was varied from 0.23 to 11.6 mM ($K_{formate}$ = 2.7 mM) with either NAD or NAD-*4-d* saturating at 20 times their K_m, an α-secondary kinetic isotope effect of 1.23 ± 0.03 was observed, but with deuterated formate the α-secondary isotope effect was reduced to 1.07 ± 0.02. Equal isotope effects were seen on V and $V/K_{formate}$. In a different type of experiment, the concentration of NAD-*4*-(H,*d*) was varied around

[4] The comparable equation when a triple label is involved, as in the use of the amino group of adenine as a remote label to determine the secondary ^{18}O isotope effect in a kinase reaction with three ^{18}O atoms in the γ-phosphate of ATP, is the same as eq 13, except that the square root becomes a cube root, the observed isotope effect is $^{15,18,18,18}(V/K)$, ^{13}k becomes ^{15}k, y is now the fraction of triply labeled species, and $1 - y$ in the last term is divided by 3, not 2.

Table V: ^{13}C Isotope Effects with Formate Dehydrogenase[a]

nucleotide	formate[c]	% reaction[d]	isotope ratios[b] ($\times 10^5$) low conversion	isotope ratios[b] ($\times 10^5$) 100% conversion	$^{13}(V/K)$[e]
NAD	H	10.0	1137.29	1183.51	1.0429
		8.7	1137.57	1183.51	1.0423
		14.8	1139.91	1183.52	1.0415
		11.2	1138.57	1183.52	1.0419
		$^{13}(V/K_{formate}) = 1.0422 \pm 0.0007$			
		$^{13}(V/K_{formate\text{-}d}) = 1.0436 \pm 0.0027$[f]			
thio-NAD	H	5.6	1141.14	1183.52	1.0382
		12.7	1142.97	1184.01	1.0385
		12.5	1143.75	1184.01	1.0377
		$^{13}(V/K_{formate}) = 1.0381 \pm 0004$			
acetylpyridine-NAD		$^{13}(V/K_{formate}) = 1.0361 \pm 0.0011$[f]			
pyridinealdehyde-NAD	H	5.5	1139.36	1184.50	1.0408
		4.2	1138.07	1184.50	1.0407
		$^{13}(V/K_{formate}) = 1.0413 \pm 0.0006$			
	D	1.1	1147.44	1194.57	1.0413
		1.1	1147.49	1194.76	1.0414
		$^{13}(V/K_{formate\text{-}d}) = 1.0414 \pm 0.0001$			
deamino-NAD	H	29.5	1143.28	1183.91	1.0425
		18.0	1140.35	1184.00	1.0423
		$^{13}(V/K_{formate}) = 1.0424 \pm 0.0001$			

[a] pH 7.8, 25 °C. Isotope effects were determined from changes in the natural abundance of ^{13}C (see Materials and Methods). [b] Ratios were adjusted for ^{17}O contribution to m/e 45 by subtracting 74 from decade settings for m/e 45/44 which were corrected to tank standard of 1260 (O'Leary, 1980). [c] H and D are unlabeled and deuterated formate. [d] Values for the low conversion samples determined by recovery of CO_2 from acidified reaction mixtures. [e] Calculated with eq 6. [f] Determined by Blanchard & Cleland (1980).

Table VI: ^{18}O Isotope Effects with Formate Dehydrogenase[a]

nucleotide	% reaction[c]	isotope ratios[b] ($\times 10^5$) low conversion	isotope ratios[b] ($\times 10^5$) 100% conversion	$^{13,18,18}(V/K)$[d]
NAD	21.0	1193.46	1246.16	1.0498
	21.0	1192.77	1246.11	1.0504
	$^{13,18,18}(V/K_{formate}) = 1.0501 \pm 0.0004$			
	$^{18}(V/K_{formate}) = 1.0049 \pm 0.0011$[e]			
thio-NAD	23.5	1195.48	1246.21	1.0486
	20.7	1193.77	1246.21	1.0494
	20.0	1194.26	1245.20	1.0481
	$^{13,18,18}(V/K_{formate}) = 1.0487 \pm 0.0007$			
	$^{18}(V/K_{formate}) = 1.0066 \pm 0.0011$[e]			
acetylpyridine-NAD	19.5	1194.13	1246.24	1.0487
	24.0	1195.24	1246.30	1.0491
	$^{13,18,18}(V/K_{formate}) = 1.0489 \pm 0.0003$			
	$^{18}(V/K_{formate}) = 1.0079 \pm 0.0014$[e]			
pyridinealdehyde-NAD	16.0	1208.31	1244.30	1.0325
	10.5	1206.84	1244.95	1.0334
	$^{13,18,18}(V/K_{formate}) = 1.0330 \pm 0.0006$			
	$^{18}(V/K_{formate}) = 0.9948 \pm 0.0004$[e]			

[a] pH 7.8, 25 °C. The substrate was a mixture of [$^{13}C^{18}O_2$] formate and [$^{12}C^{16}O_2$] formate in which the $^{13}C/^{12}C$ ratio was close to the natural abundance level (see Materials and Methods). [b] Ratios were adjusted for ^{17}O contribution to m/e 45 by subtracting 74 from decade settings for m/e 45/44 which were corrected to tank standard of 1260 (O'Leary, 1980). [c] Values for the low conversion samples determined by recovery of CO_2 from acidified reaction mixtures. [d] Calculated with eq 6. [e] Calculated from eq 13 by using the values of ^{13}k from Table V.

its K_m (32 μM) while the formate level was maintained at $0.1K_{formate}$. This type of experiment yields $^{\alpha\text{-}D}(V/K_{formate})$ as the isotope effect on both the intercept and slope of the reciprocal plots. This experiment was also repeated at 6.5 °C to investigate the temperature dependence of the α-secondary deuterium isotope effect. Analogous experiments were performed with thio-NAD, acetylpyridine–NAD, and pyridinealdehyde–NAD, and all results are in Table IV. Note that the use of deuterated formate reduces the observed isotope effect halfway from the value with unlabeled formate to the equilibrium isotope effect (0.89; Cook et al., 1980).

^{13}C Kinetic Isotope Effects. The $^{13}(V/K_{formate})$ values for each nucleotide were determined by measurement of changes in the abundance of ^{13}C during the reaction with an isotope ratio mass spectrometer. The isotope ratios together with the calculated ^{13}C isotope effects are in Table V.

^{18}O Kinetic Isotope Effects. These isotope effects were determined with the remote label method as described under Materials and Methods. The $^{13}C/^{12}C$ ratios obtained from incubations of [$^{13}C^{18}O_2$,$^{12}C^{16}O_2$]formate with formate de-

Table VII: ^{13}C and ^{18}O Isotope Effects for the I_2 Oxidation of Formate at 25 °C

mole fraction dimethyl sulfoxide	% reaction[b]	isotope ratios ($\times 10^5$)[a] low conversion 45/44	low conversion 46/44	100% conversion 45/44	100% conversion 46/44
1.00	12.0	1167.21	450.03	1184.22	447.71
	11.0	1167.48	450.80	1184.28	447.85
		$^{13}k = 1.0154 \pm 0.0001$			
		$^{18}k = 0.9938 \pm 0.0010$[c]			
0.40	10.4	1155.07	ND[d]	1184.00	ND
		$^{13}k = 1.0265$			
0	12.3	1146.22	ND	1184.12	ND
		$^{13}k = 1.0362$			

[a] Ratios were adjusted for ^{17}O contribution to m/e 45 by subtracting 74 from decade settings for m/e 45/44 which were corrected to tank standard of 1260 (O'Leary, 1980). The 46/44 ratio was corrected to a tank standard of 448. [b] Values for the low conversion samples determined by recovery of CO_2 from acidified reaction mixtures. [c] Per single oxygen since formate was natural abundance in ^{18}O and measurement was of the 46/44 ratio. [d] ND, not determined.

Table VIII: Influence of Solvent on the Rate and Isotope Effects for the I_2 Oxidation of Formate

mole fraction dimethyl sulfoxide	$k^{a,b}$ (M^{-1} s^{-1})	$^Dk^b$	$^{13}k^c$
0	1.8×10^{-2}	3.8	1.0362
0.409	2.8×10^{2}	2.9	1.0265
0.800	2.2×10^{4}	2.5	
1.000	1.0×10^{5}	2.2	1.0154

[a] Rate = $k[I_2]$[formate]. [b] Data from Hiller & Krueger (1967). [c] Data from Table VII.

hydrogenase and the various nucleotides are in Table VI, along with the ^{18}O isotope effects for a single ^{18}O substitution calculated by eq 13.

^{15}N Isotope Effects. The ^{15}N isotope effect on $V/K_{formate}$ was determined by varying the concentrations of NAD or NAD labeled with ^{15}N at N-1 of the nicotinamide ring at a fixed level of formate one-tenth of its K_m. The labeled NAD appeared to contain a competitive inhibitor, since a variable effect on the intercepts was seen, but such an inhibitor does not affect the V/K values, and isotope effects of 1.07, 1.06, and 1.07 on V/K (weighted average 1.07 ± 0.04) were seen in three experiments.

^{13}C and ^{18}O Kinetic Isotope Effects on the I_2 Oxidation of Formate. The $^{13}C/^{12}C$ ratios obtained from partial formate oxidations in 100, 40, and 0% mole fraction dimethyl sulfoxide, together with the isotope ratios for complete conversion samples and the calculated ^{13}C isotope effects, are in Table VII. The $^{18}O/^{16}O$ ratios for the partial and complete conversion reactions in pure dimethyl sulfoxide and the resulting ^{18}O isotope effect are also shown. The ^{18}O isotope effect when water was present was not determined because of the exchange of oxygen with water (it could have been determined by the remote label method with double-labeled formate). A comparison of ^{13}k and ^Dk values for this reaction as a function of solvent composition is shown in Table VIII.

^{18}O Fractionation Factors for Formic Acid and Formate. When formic acid which had been equilibrated with water at low pH was isolated as formate and converted to CO_2 with the I_2/dimethyl sulfoxide oxidizing system, an $^{18}O/^{16}O$ ratio of 0.44988% was obtained. A sample of CO_2 equilibrated with the same water had a ratio of 0.44697%. Thus, the fractionation factor of aqueous formic acid relative to gaseous CO_2 is 1.0065 ± 0.0002. Since the fractionation factor of CO_2 relative to liquid water is 1.0412 ± 0.0001 (Friedman & O'Neill, 1977), the fractionation factor of formic acid relative to water is 1.0345 ± 0.0003. Since the ^{18}O isotope effect on the ionization of formic acid is 1.0109 (Ellison & Robinson, 1983), the fractionation factor of formate ion relative to water is 1.0233. We have also used the I_2/dimethyl sulfoxide system on isolated anhydrous formate salts to determine fractionation factors for formate ion in several environments relative to formate ion in aqueous solution. These values are in Table IX.

Table IX: ^{18}O Fractionation Factors of Formic Acid and of Formate Ion in Various Environments[a]

sample	isotope ratios ($\times 10^5$)[b] reference[c] 45/44	reference[c] 46/44	sample 45/44	sample 46/44	fractionation factor[d]
formic acid	1190.91	449.88	1191.17	446.97	1.0345
sodium formate (crystal)[e]	1255.07	421.32	1256.38	421.97	1.0016
formate (on Dowex-1)[f]	1254.64	444.37	1258.02	446.24	1.0042
formate (tetrabutylammonium salt in $CHCl_3$)[g]	1254.58	444.37	1251.60	446.16	1.0040

[a] Mass ratios in formate were determined on lyophilized samples of formate salts oxidized to CO_2 by I_2 in dimethyl sulfoxide. [b] Ratios were adjusted for ^{17}O contribution to m/e 45 by subtracting 74 from decade settings for m/e 45/44 which were corrected to tank standard of 1260 (O'Leary, 1980). The 46/44 ratio was corrected to a tank standard of 448. [c] The reference material was the residual formate in solution in equilibrium with the sodium formate crystal, the Dowex-1 resin, or the chloroform layer, except for the case of formic acid, where it was CO_2 equilibrated with the same water with which formic acid had been equilibrated. [d] Relative to water for formic acid (corrected for the fractionation factor of CO_2 gas relative to water, 1.0412; Friedman & O'Neill, 1977); relative to formate ion in aqueous solution in the other cases. [e] Crystals were grown over 1 h and stirred for 4 days (about 5% of the material crystallized). The crystals were filtered, and the residual solution was lyophilized. [f] Dowex 1-X8-Cl was stirred with a solution containing a 10-fold excess of sodium formate for 4 days. The resin was filtered off, washed extensively with water, and eluted with 1 N NaOH; it had been half-saturated with formate. The eluted formate and residual formate solutions were lyophilized. [g] Sodium formate (1 g) and 300 mg of tetrabutylammonium bromide in 5 mL of water were partitioned against 45 mL of $CHCl_3$. The two phases were stirred overnight, and the $CHCl_3$ layer was separated and evaporated to dryness. The aqueous layer was lyophilized. The tetrabutylammonium ion did not interfere with the I_2 oxidation.

Discussion

Formate dehydrogenase is particularly amenable to heavy-atom isotope effect study since the product, CO_2, is ideally suited for isotope ratio mass spectrometric analysis. Since the ^{13}C isotope effect was the same with deuterated and unlabeled formate, Blanchard & Cleland (1980) deduced that the hydride transfer step was totally rate limiting, and thus there were no commitments for this reaction.[5] We have confirmed this with pyridinealdehyde–NAD in the present

[5] For most dehydrogenases steps other than hydride transfer are at least partially rate limiting, so that the observed isotope effect on V/K is reduced by forward and/or reverse commitments, which are defined as the ratio of the rate of hydride transfer to the net rate constant for release of a reactant from the enzyme. The reactant whose rate of release determines the forward commitment is the variable substrate in a direct comparison experiment or the labeled one in an internal competition experiment (as here with natural abundance ^{13}C labels), while the rate of release of the first product determines the reverse commitment. See Cook & Cleland (1981) for a more complete description of isotope effect theory.

work. The absence of commitments greatly simplifies analysis of the isotope effects, since the values observed are the intrinsic ones on the hydride transfer step. We will assume that all isotope effects reported in the present work are intrinsic values on hydride transfer, except for the ^{15}N isotope effect [which by analogy with what has been deduced for the alcohol dehydrogenase reaction by Cook et al. (1981) may be on a step prior to hydride transfer, so that one would observe the equilibrium isotope effect on this step], and that portion of the ^{18}O isotope effects which appears to result from equilibrium isotope effects on the dehydration of formate during binding.

Correlation of Isotope Effects with Transition-State Structure. The primary deuterium isotope effects increase as nucleotide redox potential is increased and the reaction becomes more thermodynamically favored (Table III). Hammond's postulate states that such a thermodynamic change will result in an earlier transition state (Hammond, 1955). A change to an earlier transition state with an increase in primary deuterium isotope effect suggests that the transition state for NAD is productlike, or later than symmetrical (Westheimer, 1961).

The ^{13}C isotope effects (Table V) decrease through the series from NAD to acetylpyridine–NAD, indicating that C–H bond cleavage is less advanced with the more redox positive nucleotide and the transition state is earlier (the apparently anomalous ^{13}C isotope effect for pyridinealdehyde–NAD will be discussed). The redox potential of deamino-NAD (modification on the adenine ring) is identical with that of NAD, and the similarity of the ^{13}C and deuterium isotope effects and V_{max} values for NAD and deamino-NAD suggests that the transition state for the latter is similar to that for NAD.

The trends in both deuterium and ^{13}C isotope effects thus both support the idea that the transition state is earlier and more symmetrical with acetylpyridine–NAD than with NAD. The data for the I_2 oxidation of formate by contrast appear to cover the range from early to near-symmetrical transition states (Table VIII). In pure dimethyl sulfoxide the low values of both ^{13}k and ^{D}k suggest an early transition state. As the proportion of water in the solvent increases, the rate drops drastically (nearly 7 orders of magnitude in pure water), and both ^{D}k and ^{13}k increase, with the value of ^{13}k in water being the same as from the enzymatic oxidation by acetylpyridine–NAD. It thus appears that the I_2 oxidation covers one limb of the Westheimer curve and the enzymatic oxidation the other. To our knowledge this study and that in the previous paper (Scharschmidt et al., 1984) are the first examples where ^{13}C isotope effects have been determined as a function of transition-state structure, although the oxidation of formate by carbonium ions of various redox potentials does show a Westheimer curve for the deuterium isotope effects (Stewart & Toone, 1978).

While the I_2 oxidation of formate does show the drastic change in rate with change in transition-state structure predicted by the theory of Marcus (1968), the trend in the rates of the enzymatic reaction is the reverse of that expected; that is, NAD is the fastest substrate, and acetylpyridine–NAD is much slower. Further, the redox potential of NAD is −0.32 V, while that of formate is −0.42 V, so that if these reactants had the same redox potentials in their ternary complexes with the enzyme, the transition state would be predicted to be early, rather than late. Clearly the enzyme is having an effect on the transition-state structure (and presumably on redox potentials), although how this is done is not clear. It is intriguing that both with liver alcohol dehydrogenase [see Scharschmidt et al. (1984)] and with formate dehydrogenase the transition state with the natural substrate NAD is somewhat late, although benzyl alcohol has a redox potential *higher* than that of NAD and formate has one that is *lower*.[6] What is clear, however, is that despite these influences, using a nucleotide with a more positive redox potential than that of NAD makes the enzymatic transition state earlier and apparently more symmetrical. A full interpretation of transition-state structure will have to await the measurement of ^{13}C isotope effects at the 4-position of the nucleotide, the technology for which is under development.

Inhibition by Azide and Nitrate. Azide is a linear molecule resembling CO_2 and nitrate a trigonal one resembling formate, and Blanchard & Cleland (1980) suggested that azide, because it bound much more tightly to the E–NAD complex than either formate or nitrate, was acting as a transition-state analogue. We thus felt that the relative K_i values of azide, nitrate, and formate with different nucleotide substrates might help to define the variation in transition-state structure. It is clear from the data in Table II that NAD induces much tighter binding of all three molecules than do the other nucleotide substrates. Azide does bind more loosely as the redox potential of the nucleotide gets more positive, but the trend in $K_{formate}$ and $K_{i\ nitrate}$ values is nearly the same, showing that the alternate nucleotide substrates are failing to induce as efficiently as NAD the conformation changes that lead to formation of the binding pocket for formate. This failure also causes the observed decrease in V/K values with the alternate nucleotides, which is in the opposite direction from that expected from the redox potentials alone. We conclude that while the binding pocket for formate shows a tighter affinity for a linear anionic molecule than for a trigonal one and this may contribute to catalysis, the structure is not different for the different enzyme–nucleotide complexes.

Interpretation of ^{18}O Isotope Effects. The ^{18}O isotope effects reported in Table VI are the first such values to be measured for a decarboxylation reaction. If the isotope effect is considered purely as a secondary one, it should be inverse, since the estimated equilibrium isotope effect is 0.983 (the bond order to the oxygen is 2.0 in CO_2 but only 1.5 in formate). The I_2 oxidation of formate in dimethyl sulfoxide, which we believe to have an early transition state, does show a small inverse ^{18}O isotope effect of 0.9938 in agreement with this prediction. On the other hand, if motion of the oxygens is part of the reaction coordinate motion, this could produce a normal isotope effect, as is clearly the case for the ^{13}C isotope effects. We believe this is not an important contribution for the ^{18}O isotope effects because the oxygens remain bonded to the same atom during the reaction and because most of the heavy atom motion during the reaction is that of the carbon. Conversion of formate to CO_2 requires the carbon to become collinear with the oxygens, and since they have a mass of 32

[6] It is possible that formate is not absorbed simply as the counterion to the positive charge of the nicotinamide ring of NAD but rather that its binding pocket has an arginine or lysine present in it to strengthen binding of formate. While this positive charge would facilitate binding of formate, it would depress the rate of hydride transfer and thus possibly explain why such an apparently strongly exergonic chemical reaction is totally rate limiting for the overall enzymatic reaction. This positive charge would certainly raise the redox potential of formate, although whether it could raise it sufficiently to produce a late transition state with NAD is not clear. A possible perturbation in redox potential of the nucleotide could result from geometric deformation on binding or as the result of conformation changes after binding. Pyramidalization of N-1 would certainly raise the redox potential, while twisting of the side chain out of the plane of the nicotinamide ring would lower it drastically. Unfortunately, X-ray studies have not yet been carried out with formate dehydrogenase.

and it has a mass of 12, most of the motion is by the carbon.

Three of the measured ^{18}O isotope effects are, however, normal, although they do become less normal as the redox potential of the nucleotide becomes more negative, as predicted (we will discuss the one inverse value with pyridinealdehyde–NAD below). In the above discussion we have not considered the ^{18}O isotope effect that would accompany the dehydration of formate during its binding to the enzyme–nucleotide complex. The ^{18}O vapor pressure isotope effect for water is 1.0091 (Szapiro & Steckel, 1967); that is, the hydrogen bonds in liquid water increase the bonding to the oxygen sufficiently to cause nearly a 1% fractionation factor between the vapor phase and the liquid. An effect at least this large is expected for desolvation of formate ion in aqueous solution, since each oxygen which carries a half negative charge can form up to three hydrogen bonds, as opposed to the two that an oxygen in water may participate in. We attempted to measure this effect by determining the ^{18}O fractionation factor of formate in the sodium formate crystal which contains no water, but as the data in Table IX show, the close proximity of the oxygens to the positive charges in the crystal stiffens the vibrational frequencies of the oxygens sufficiently to overcome the dehydration isotope effect (we presume this is simply the result of the half negative charge oscillating in the near vicinity of the positive charges; both stretching and bending frequencies should be elevated by the effect). This ion pairing isotope effect is also seen in the fractionation factors of formate bound as the counterion to Dowex-1 resin or partitioned into $CHCl_3$ as the tetrabutylammonium salt (Table IX). In both of these cases we believe that formate is still hydrated, so that the fractionation is almost solely an ion pairing effect. We conclude that formate is thus bound to the enzyme–nucleotide complex in such a way that it is dehydrated but not bound as a tight ion pair (that is, it is probably bound as the counterion to the positive charge on N-1 of the nicotinamide ring of NAD, which is far enough removed from C-4 that the vibrational frequencies of the oxygens of formate are not appreciably affected). The observed ^{18}O isotope effects are thus the product of an equilibrium dehydration isotope effect of 1.01–1.02 and a kinetic isotope effect which is probably inverse but is certainly less inverse for nucleotides with more positive redox potential.

The one exception to the above trends is pyridinealdehyde–NAD, which gives an inverse ^{18}O isotope effect. It is also a very slow substrate, and it is tempting to postulate that the conformation change which sets the stage for hydride transfer does not completely dehydrate formate in this case. We also believe the reaction coordinate for hydride transfer with this nucleotide is longer than with the better substrates as the result of this defective conformation change. Thus, the ^{13}k value is as high as with NAD, and the activation energy for both V and V/K is considerably higher than for the faster substrates (Table I). On the basis of all of the isotope effects reported here, we postulate transition-state structures like those shown diagrammatically in Figure 2 for the various nucleotides.

α-Secondary Deuterium Isotope Effects. In studies with liver and yeast alcohol dehydrogenases, Cook et al. (1981) found that intrinsic α-secondary isotope effects using NAD-*4-d* were normal from the NAD side (1.22 with 2-propanol and the yeast enzyme and 1.34 for cyclohexanol and the liver enzyme) while the equilibrium isotope effect is 0.89 (Cook et al., 1980). Thus, they concluded that the α-secondary hydrogen in the transition state is more loosely bonded than in either NAD or NADH as the result of coupling of the

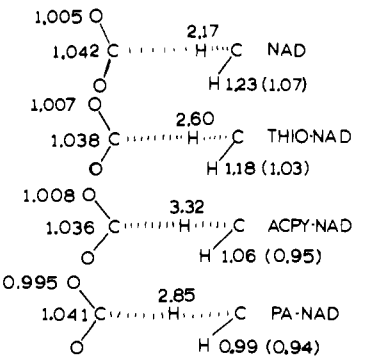

FIGURE 2: Diagrammatic representation of the variation in transition-state structure with change in nucleotide. ACPY–NAD and PA–NAD refer to acetylpyridine–NAD and pyridinealdehyde–NAD. The observed isotope effects for each atom are shown (the values in parentheses for α-secondary deuterium substitution are for deuterated formate).

translational motion of the hydrogen undergoing hydride transfer and the bending motion of the α-secondary hydrogen in the transition state. The force constant for the out-of-plane bending mode of the α-secondary hydrogen (see Figure 1) is thus greatly reduced (or negative) in the transition state, and the observed isotope effects reflect the loss, or near loss, of this vibrational mode (Cook et al., 1981).

With formate dehydrogenase, similar normal α-secondary deuterium isotope effects are seen with NAD, thio-NAD, and acetylpyridine–NAD, and only with pyridinealdehyde–NAD is the value slightly inverse (Table IV) The bending motion of the α-secondary hydrogen thus appears more tightly coupled to the hydride transfer with those nucleotide substrates with later transition states. The low value for pyridinealdehyde–NAD may reflect a stretched reaction coordinate (that is, rather long distance between C-4 of the nucleotide and the hydride) or simply inefficient coupling of hydrogen motions for this slow reaction. It seems intuitively reasonable that the coupling of hydrogen motions would be tighter in a transition state where the hydride hydrogen was closer to C-4 of the nucleotide, but a good theoretical model for this situation does not exist.

When deuterated formate was used in these experiments, the α-secondary deuterium isotope effect in each case was reduced halfway to the equilibrium isotope effect, even with pyridinealdehyde–NAD. Similar effects have been seen in model hydride transfer reactions by Ostović et al. (1983), who obtained $^{\alpha\text{-D}}k$ values of 1.11 and 0.98 for the reduction of 10-methylacridinium or its 9-deuterated analogue by 5,6-dihydro-5-[4-(trifluoromethyl)benzyl]phenanthridine and its 6-dideuterio analogue. Other cases of coupled hydrogen motions in which the isotope effects differ for the first and second deuterium substitution include the motions of hydrogens in the central hole of *meso*-tetraphenylporphine (an isotope effect of 10 for the first deuterium substitution and 1.0 for the second) and the interchange of hydrogens in the cyclic complex of acetic acid and methanol in tetrahydrofuran (isotope effects of 5.1 and 3.1 for the first and second deuterium substitutions) (Limbach et al., 1982). Enzymatic examples are the glucose-6-P dehydrogenase reaction, which gives a primary deuterium isotope effect of 5.3 in H_2O and of 3.7 in D_2O where the proton whose motion is coupled to hydride transfer is a deuteron (J. D. Hermes and W. W. Cleland, unpublished experiments), and the dehydrogenation of 5,10-methylenetetrahydrofolate, where the observed primary deuterium isotope effect is reduced from 1.70 to 1.55 when the α-secondary position is also deuterated (Farina et al., 1973).

This drastic effect of deuterium substitution on another deuterium isotope effect shows clearly that the motions of the two hydrogens are coupled in the transition state, but this coupling alone will not account for the phenomenon. Theoretical work (Limbach et al., 1982; Huskey & Schowen, 1983; Saunders, 1984) shows that this effect is seen only when quantum mechanical tunneling is involved. Where two hydrogens are moving at the same time in the reaction coordinate, H + H tunnel efficiently, but H + D or D + D do not, so that the second deuterium substitution causes a smaller isotope effect. To model this situation, Huskey & Schowen (1983) and Saunders (1984) have found it necessary to assume imaginary frequencies of at least 1000 cm^{-1}, which correspond to a narrow barrier with a high degree of curvature. We thus conclude that the α-secondary deuterium isotope effects for formate dehydrogenase establish that tunneling is involved in the hydride transfer process, even for the slower substrates. This conclusion should come as no surprise, since a reaction which proceeds by tunneling will be faster and have a lower activation energy than one with a higher and broader barrier. Compression along the reaction coordinate by the enzyme, as well as optimizing the geometry of the reactants, would certainly facilitate such a situation, although it must be remembered that similar tunneling appears to be involved in the nonenzymatic hydride transfer reactions observed by Ostovič et al. (1983). Powell & Bruice (1983) have also concluded from the temperature variation of deuterium isotope effects that model hydride transfer reactions involve tunneling. We suspect that all dehydrogenase reactions will be found to involve tunneling and hope that further theoretical work will better define the factors involved in these reactions.

^{15}N Isotope Effect. Cook et al. (1981) found that NAD labeled at N-1 of the nicotinamide ring with ^{15}N gave an isotope effect with liver alcohol dehydrogenase and cyclohexanol of 1.06 which exceeded the equilibrium isotope effect, suggesting that this nitrogen has a bond order of 3 at some point in the reaction prior to hydride transfer. They postulated that geometric distortion of the nicotinamide ring (most likely to a boat form similar to that shown in Figure 1) to make N-1 pyramidal produced a carbonium ion at C-4 which induced hydride transfer. This distortion is readily brought about by movement of C-5 and C-6 out of the plane of the nicotinamide ring (presumably as the result of forces brought to bear by the enzyme during the conformation change that sets the stage for hydride transfer). These studies used the equilibrium perturbation method of measuring the isotope effect (Schimerlik et al., 1975), which works only for a reversible reaction. We have used the direct comparison method which is less accurate, but the weighted average of three determinations of $^{15}(V/K)$ was 1.07 ± 0.04, and thus a similar ^{15}N isotope effect is seen for formate dehydrogenase as the one reported for alcohol dehydrogenase. Since there are no commitments for the formate dehydrogenase reaction, we cannot tell whether this is a kinetic isotope effect on the hydride transfer step or an equilibrium isotope effect on a step prior to hydride transfer, but we can say that the same geometric distortion that produces carbonium ion character at C-4 in the alcohol dehydrogenase reaction appears to be involved here and is probably a general catalytic mechanism for all dehydrogenases.

References

Biellmann, J. F., & Jung, M. J. (1970) *FEBS Lett. 7*, 199.

Blanchard, J. S., & Cleland, W. W. (1980) *Biochemistry 19*, 3543.

Cleland, W. W. (1979) *Methods Enzymol. 63*, 103.

Cook, P. F., & Cleland, W. W. (1981) *Biochemistry 20*, 1790.

Cook, P. F., Blanchard, J. S., & Cleland, W. W. (1980) *Biochemistry 19*, 4853.

Cook, P. F., Oppenheimer, N. J., & Cleland, W. W. (1981) *Biochemistry, 20*, 1817.

Ellison, S. L. R., & Robinson, M. J. T. (1983) *J. Chem. Soc., Chem. Commun.*, 745.

Farina, P. R., Farina, L. J., & Benkovic, S. J. (1973) *J. Am. Chem. Soc. 95*, 5409.

Friedman, I., & O'Neill, J. R. (1977) *Geol. Surv. Prof. Pap. (U.S.) No. 440-KK*.

Hammond, G. S. (1955) *J. Am. Chem. Soc. 77*, 334.

Hiller, F. W., & Krueger, J. H. (1967) *Inorg. Chem. 6*, 528.

Huskey, W. P., & Schowen, R. L. (1983) *J. Am. Chem. Soc. 105*, 5704.

Limbach, H.-H., Hennig, J., Gerritzen, D., & Rumpel, H. (1982) *Faraday Discuss. Chem. Soc. 74*, 229.

Northrop, D. B. (1977) in *Isotope Effects on Enzyme-Catalyzed Reactions* (Cleland, W. W., O'Leary, M. H., & Northrop, D. B., Eds.) p 122, University Park Press, Baltimore.

O'Leary, M. H. (1980) *Methods Enzymol. 64*, 83.

O'Leary, M. H.; & Marlier, J. F. (1979) *J. Am. Chem. Soc. 101*, 3300.

Ostovič, D., Roberts, R. M. G., & Kreevoy, M. M. (1983) *J. Am. Chem. Soc. 105*, 7629.

Powell, M. F., & Bruice, T. C. (1983) *J. Am. Chem. Soc. 105*, 7139.

Risley, J. M., & van Etten, R. L. (1980) *J. Am. Chem. Soc. 102*, 4609.

Saunders, W. H., Jr. (1984) *J. Am. Chem. Soc. 106*, 2223.

Scharschmidt, M., Fisher, M. A., & Cleland, W. W. (1984) *Biochemistry* (preceding paper in this issue).

Schimerlik, M. I., Rife, J. E., & Cleland, W. W. (1975) *Biochemistry 14*, 5347.

Stewart, R., & Toone, T. W. (1978) *J. Chem. Soc., Perkin Trans. 2*, 1243.

Szapiro, S., & Steckel, F. (1967) *Trans. Faraday Soc. 63*, 883.

Viola, R. E., Cook, P. F., & Cleland, W. W. (1979) *Anal. Biochem. 96*, 334.

Westheimer, F. H. (1961) *Chem. Rev. 61*, 265.